微波溶剂热法制备掺氮石墨烯用于碱性氧还原反应

程 铭 史瑞娜 刘树森 赵金仙 任 军*
(太原理工大学煤科学与技术重点实验室, 太原 030024)

摘要：采用微波处理氧化石墨烯(GO)与乙二醇(EG)、乙二胺(ED)混合液的方法制备氮掺杂石墨烯(NG)，使用旋转圆盘电极对 NG 催化氧还原在碱性溶液中反应进行研究，并考察了不同微波辐射时间、ED 与 EG 之比对反应性能的影响。采用 X 射线衍射仪 (XRD)、透射电子显微镜(TEM)、拉曼光谱(Raman)和傅里叶变换红外光谱(FT-IR)研究了 NG 催化剂的结构与性质。相比于未掺氮 的石墨烯样品，NG 表现出更正的起始电位和接近四电子的转移过程。NG 中掺杂氮原子的键合方式通过 XPS 进行表征，结果表 明起始电位的高低取决于石墨氮含量。此外，所有表征结果表明总氮含量与氧还原反应性能没有直接关系。

关键词：微波溶剂热；氧还原反应；石墨氮；氮掺杂石墨烯

Nitrogen-doped Graphene by Microwave Solvothermal for Oxygen Reduction Reactions in Alkaline Electrolyte

CHENG Ming SHI Rui-Na LIU Shu-Sen ZHAO Jin-Xian REN Jun*
(*Key Laboratory of Coal Science and Technology Taiyuan University of Technology,*
Ministry of Education and Shanxi Province, Taiyuan 030024, *China*)

Abstract: Nitrogen-doped graphene (NG) catalyst on the oxygen reduction reaction (ORR) has been investigated in alkaline solution using the rotating disk electrode (RDE) method. Here, we reported a facile NG catalyst via a convenient and simple method of microwave solvothermal from graphite oxide (GO) in the mixture solution of ethylene glycol (EG) and ethylene diamine (ED). The effect of microwave irradiation time and the ratio of EG and ED on the performance of the catalyst were investigated. The structure and property of NG catalysts were characterized by X-ray diffraction (XRD), Transmission electron microscopy (TEM), Raman spectroscopy, and Fourier transform infrared spectra (FT-IR). Most importantly, the as-synthesized NG catalyst exhibited a positive onset potential (E_{ORR}) and nearly four electron transfer process, which is better than non-N-graphene. Furthermore, the role of various nitrogen states in NG catalysts were investigated by X-ray spectroscopy (XPS), and the results showed that the content of graphite-N components determined the E_{ORR}. Besides, comprehensive characterizations revealed that NG catalyst in ORR process had no direct relationships with the content of total N.

Keywords: microwave solvothermal; oxygen reduction reaction; graphite-N; nitrogen-doped grapheme

0 Introduction

Recently, fuel cell as a new renewable energy has been widely concerned. The electrochemical performance of a fuel cell depends largely on oxygen reduction reaction (ORR)[1-2]. Due to its overpotential and high current density, platinum-based catalyst has been commercially applied in fuel cell[3-4]. However, its

application was limited by resource scarcity, high cost, crossover, and poisoning effects[5-9]. Hence, more and more researchers dedicated to develop non-noble metal catalyst for ORR[10-12]. Previous studies have revealed that pyrolysis N_4-macrocyclic exhibit superb performance in ORR, but stability issue arose as the damage of catalyst structures in the acidic medium[13] which hinders its practical application. Nowadays, various kinds of non-metal carbon-based materials have attracted more and more concern for fuel cell as catalyst, such as graphite carbon[14], carbon nanotubes (CNTs)[15], carbon fiber[16], graphene. Among above materials, graphene has attracted more attention for its large specific surface area, good electrical conductivity and special two-dimensional structure[17]. However, pristine graphene does not show any performance in ORR because it does not exist band gap [18]. Chemical doping with heteroatoms (boron[19], sulfur[20], phosphor[21]) turns out to be an effective approach to achieve excellent electrocatalytic activity for ORR, which has been proved by both theoretical calculations and experiments. We noticed that there were only a few reports focusing on the synthesis of B-, P-, S-graphene due to the harsh conditions in synthesis and atom size are disunity, so less content of doped obtained. Nitrogen doped graphene (NG) materials can be obtained by replacing carbon atom with nitrogen atom in graphene frameworks. The NG shows different properties compared with the pristine graphene. Such as, the charge distribution and spin density of C atoms will be influence by the neighbor N[22-23], N atoms doping creates positive charge sites due to higher electronegativity than carbon (2.25), which induces the "activation region" on the surface of graphene can participate in ORR[24], and this results in great improvement of electrocatalytic performance. Compared to Pt-based catalysts, NG has similar overpotential, excellent long-term stability, low cost and the similar chemical nature[25]. Furthermore, NG material has different N species with variety electronic structure. Previous studies have shown that graphite-N is a major factor for ORR[26]. Hence, NG catalyst is highly promising to replace Pt-based material.

Recently, various techniques such as chemical vapor deposition (CVD)[27], solvothermal[28], thermal polymerization[29], and plasma[30] were used to synthesis NG material. Among above all, solvothermal method was widely proposed to synthesis NG by using ammonium hydroxide or urea as nitrogen source, and the maximum value of N atomic percentage 10.1%[12]. However, time-consuming and the low production efficiency hindered the development of solvothermal. Microwave solvothermal can overcome the limitation which achieved effective energy saving and environment protection for traditional method because the centers on dielectric microwave heating[31] of the reactants by transferring energy selectively can be short the reaction time. Currently, microwave solvothermal has been widely applied in the field of material and thin film preparation. The NG samples were prepared successfully by Wang et al.[32] with a low nitrogen mass percentage (5.47%) showed E_{ORR} of 0.17 V (vs Hg/HgO) via microwave heating of graphene oxide under NH_3 flow in just ten seconds. However, the numbers of electrons transferred per oxygen molecule (n) were 3.03~3.30 which may indicate more intermediate products.

In this paper, we report an innovation, rapid and convenient synthesis strategy for NG material by microwave solvothermal. Ethylene diamine (ED), a well-known short chains organic amine to reduce epoxy functional[33], was selected as the nitrogen source in our work. The atomic percentage of total nitrogen sample up to 7.46% can be obtained and selected as the optimal sample in short ten minutes, which was more than reported before. Moreover, the sample exhibited favorable electrons transferred process of per oxygen molecule (n) (3.50) at −0.35 V.

1　Experimental

1.1　Materials and synthesis of NG

1.1.1　Materials

Potassium hydroxide (KOH, AR, 85%) was purchased from Tianjin Kemiou Chemical Reagent Co. Ltd. Graphene oxide (GO, 99%) which was a commercial product obtained from Institute of Coal Chemistry,

Chinese Academy of Science. Ethylene diamine (ED, AR, 99%) and Ethanol (EtOH, AR, 99%) used for all experiments was obtained from Tianjin Zhiyuan Chemical Reagent Co. Ltd. Ethylene glycol (EG, AR) was purchased from Tianjin Hengxing Chemical Reagent Co. Ltd). Nafion (mass percentage 5%) was purchased from Dupont Chemical Reagent Co. Ltd. Alumina powders (0.5 μm) used for all experiments was obtained from Zhejiang Wuyihengyu Instrument Co. Ltd.

1.1.2　Synthesis of the catalysts

The NG catalysts were prepared by microwave solvothermal process. In a typical synthesis (Scheme 1), graphene oxide (GO) was added to the mixture solution of EG and ED (1:1, *V/V*). After ultrasonicated

for 30 min, the mixture was heated to 180 ℃ with a rate of 16 ℃·min⁻¹ in the microwave reactor with the power of 350 W when rotating in a speed of 600 r·min⁻¹. Then After kept for several minutes, the reactor naturally cooled down to 55 ℃. The products were taken out, centrifuged and washed with deionized water for three times to remove residual ammonia solution. Finally, the samples were dried at 70 ℃ overnight under vacuum, and then, the NG samples with different microwave irradiation times were obtained.

The catalysts were prepared using EG and ED with different ratios (1:0, 3:1, 1:1, 1:3, 0:1; *V/V*) at 180 ℃ for 10 min, and were denoted as NG-1, NG-2, NG-3, NG-4, and NG-5, respectively.
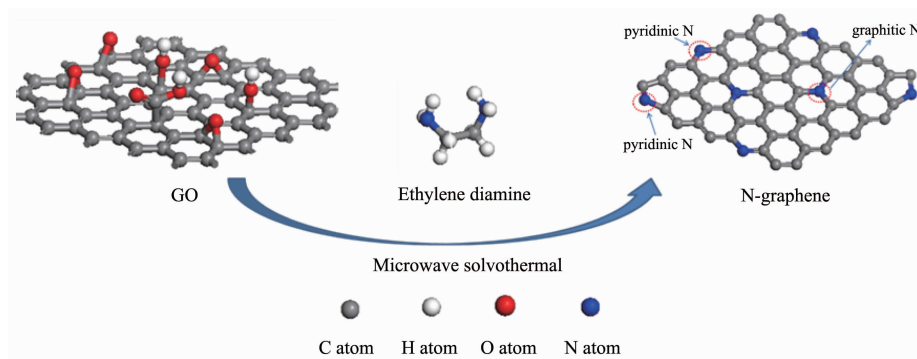
Scheme 1　Illustration of the preparation procedure of NG

1.2　Sample characerizations of NG and electrochemical measurements

1.2.1　Sample characterizations

The powder X-ray diffraction (XRD) measurement was performed on a Rigaku D/max 2500 with Cu *Kα* (*λ*=0.154 056 nm) radiation and a graphite monochromator operated at 40 kV and 100 mA. The range of X-ray diffractometer with 2*θ* was from 5° to 85°. The Bragg diffraction equation (2*d*sin*θ*=*nλ*) was used for the calculation of interlayer space of all samples.

The microscopic features such as morphology and layer structure of graphene were observed using transmission electron microscopy (TEM) (JEM-2010F, JEOL, Japan) under 200 keV. The samples for TEM measurements were prepared by dispersing the products in ethanol using an ultrasonic bath for 10

min, and then, a drop of the suspension was placed on a carbon-coated copper grid at room temperature.

The graphitization degree of carbon materials can be characterized by Raman spectrometer (Renishaw 21000) with a 514.5 nm wavelength Ar⁺ laser. The scanning range was from 100 to 3 200 cm⁻¹ at the step length of 1 cm⁻¹.

Fourier transform infrared (FT-IR) spectra for characterizing functional groups in samples were recorded using on a TENSOR27 spectrometer technique ranging from 400 to 4 000 cm⁻¹. FT-IR test of the samples was prepared by fully grounding the mixture of 2 mg powdered samples and 80 mg KBr. Before used, the KBr was dried at vacuum overnight.

Various nitrogen content and states in NG samples can be distinguished by X-ray photoelectron spectroscopy (XPS). The data were collected on a V.G

Scientific ESCALAB250Xi using 300 W Al $K\alpha$ radiation ($h\nu$=1 486.6 eV). The binding energies were referenced to the C1s line at 284.6 eV from adventitious carbon.

1.2.2 Electrochemical measurements

The electrochemical measurements were performed on CHI 660 E with a standard three-electrode system. In a typical three-electrode system, the glass-carbon (GC, with 5 mm diameter) electrode was used as the working electrode; a Pt foil and Ag/AgCl (saturated KCl) were used as counter and reference electrodes, respectively. To prepare working electrode, firstly, GC electrodes were pretreated on a polishing cloth using 0.5 μm alumina slurries, after polishing, the electrodes were sonicated followed by HNO_3 (V_{HNO_3}:V_{H_2O}=1:2), EtOH, and deionized water in turn to remove alumina residues. Subsequently, a certain amount mixture of NG, EtOH, deionized water and Nafion solution as a binder sonicated for 30 min. Then, 10 μL of sonicated suspension was dropped on the pretreated working electrode by micropipet tip, dried in air and dried furtherly under infrared lamp. The NG loading calculated was 277.94 μg·cm⁻².

The linear-scan-voltammetry (LSV) measurements were performed on a rotation disk electrode (RDE) using 0.1 mol·L⁻¹ KOH aqueous solution with saturation oxygen between −1.0 V and 0.0 V (vs Ag/AgCl), and then subtracted the background under N_2-saturated. Koutechy-Levich (K-L) plots were analyzed at various rotation speeds (400, 800, 1 200 and 1 600 r·min⁻¹). The slopes of linear fit lines were used to calculate the number of electrons transferred per oxygen molecule (n) on basis of the K-L equation:

$$\frac{1}{J}=\frac{1}{J_k}+\frac{1}{B\omega^{1/2}}$$

$$B=0.2nFC_0(D_0)^{1/2}(\nu)^{-1/6}$$

J, J_k are the measured current density and kinetic-limiting current density, respectively. ω is the rotation speed in r·min⁻¹; n is the number of transferred electrons for per oxygen molecule; F is the Faraday constant (96 485 C·mol⁻¹); D_0 is the diffusion coefficient of oxygen in 0.1 mol·L⁻¹ KOH (1.9×10⁻⁵ cm·s⁻¹); ν is the kinetic viscosity (0.01 cm²·s⁻¹); C_0 is the bulk concentration of oxygen (1.2 μmol·cm⁻³); 0.2 is a cons-tant when the rotation speed expressed in r·min⁻¹.

2 Results and discussion

2.1 Characterizations

2.1.1 XRD analysis

The XRD patterns of GO, NG-1, NG-2, NG-3, NG-4 and NG-5 samples were exhibited in Fig.1. As shown in Fig.1, GO has a sharp diffraction peak around 11.6° which is corresponding to the characteristic facets of (002). The interlayer space calculated from Bragg diffraction equation was 0.760 nm (d_{002} of ~0.760 nm). The diffraction peak completely disappeared after microwave solvothermal which can be attributed to the deoxidization of oxygen functional groups. Furthermore, all of NG-1, NG-2, NG-3, NG-4 and NG-5 have a broad diffraction peak appeared at around 24.5°, corresponding to interlayer space of around 0.374, 0.361, 0.360, 0.370 and 0.366 nm, which indicated that the few-layer stacked appears on frameworks of graphene nanosheets[34]. Single-crystal structure of graphitic (d_{002} of ~0.335 nm) was recovered as well[35].
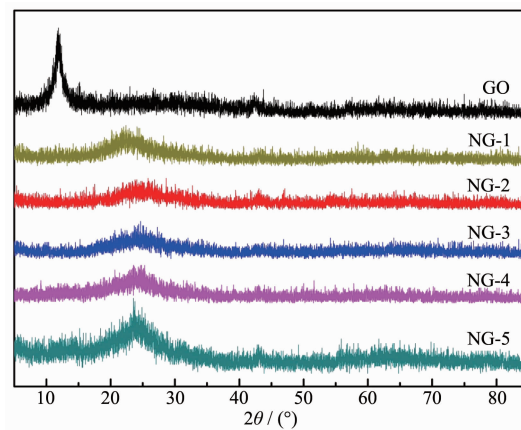

Fig.1 XRD patterns of GO, NG-1, NG-2, NG-3, NG-4 and NG-5 samples

2.1.2 TEM analysis

Morphologies details of all NG catalysts were characterized by TEM. As shown in the low-magnification TEM image (Fig.2), the NG nanosheets had a typical crumpled surface with random stacking, which might be attributed to the defective structure, distortion of graphene formed upon exfoliation and the presence of foreign N atoms[10]. Furthermore, TEM

images showed that NG contained only a few layers of graphene sheets. This suggests that the NG samples had a similar layer structure to graphene and the layer number of the NG was quite low. The image of high-resolution transmission electron micrograph (HRTEM) revealed that the NG was well-crystallized and the graphitic layer with a (002) crystal plane corresponding to lattice spacing of 0.36 nm appear clearly (Fig. 2d), which is closer to that of single-crystal graphite (0.335 nm). Moreover, it is clear that NG-1, NG-2, NG-4 and NG-5 are more crumple than NG-3. The results strongly support the viewpoint that the suitable proportion of EG and ED is the essential reasons to prepare low layer numbers NG.
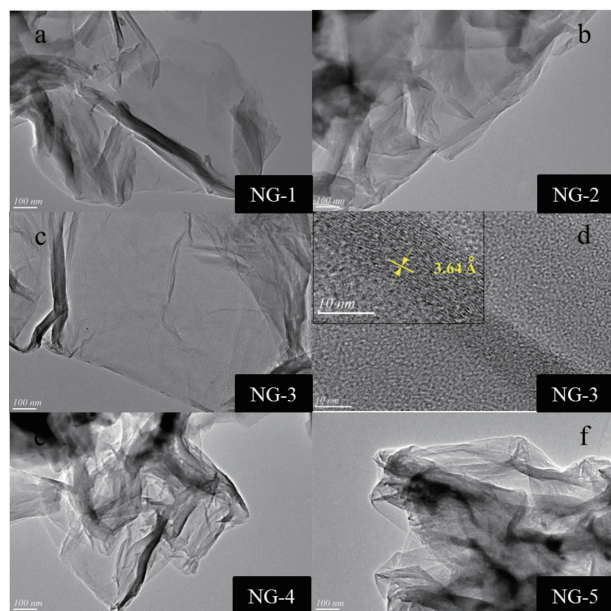

Fig.2　TEM images of (a) NG-1, (b) NG-2, (c) (d) NG-3, (e) NG-4, and (f) NG-5

2.1.3　Raman spectroscopy analysis

Raman spectroscopy is the most direct and nondestructive technique to characterize the structure and quality of carbon materials[36], particularly to determine the defects, the degree of graphitization, and the layers of graphene. The Raman spectra of NG exhibit two remarkable peaks at around 1 350 and 1 590 cm^{-1} (Fig.3), corresponding to the well-defined D band and G band, respectively. Generally speaking, the D band is associated with structural defects and partially disordered structures[37], while the G band is

related to the E_{2g} vibration mode of sp^2 carbon domains can be used to explain the degree of graphitization. The structural defects represented by the values of I_D/I_G which were calculated from Fig.3 and listed in Table 1. It is clearly that the I_D/I_G value of the NG-1 (0.96) is lower than others N doped samples (I_D/I_G= 1.06 ~1.16). The results indicated that N atoms successfully doped into the graphene skeleton through microwave solvothermal, inducing the formation of more defect and the decomposition of oxygen-containing groups within the GO structure. The values of I_D/I_G are depended on the amount of N doped, so it indicated that more N atoms doped result in more defect formed in graphene.
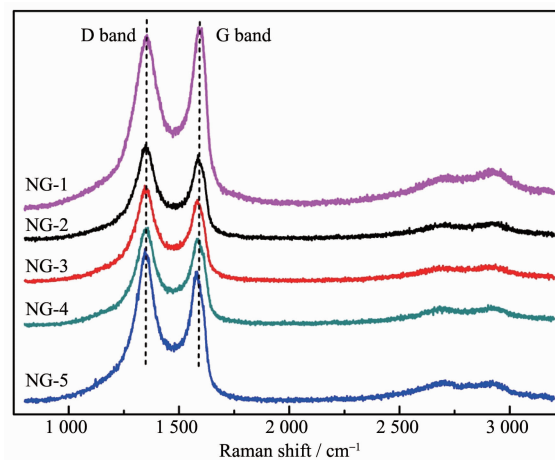

Fig.3　Raman spectra of NG-1, NG-2, NG-3, NG-4 and NG-5 samples

Table 1　Values of I_D/I_G with NG-1, NG-2, NG-3, NG-4 and NG-5 samples

Sample	N atomic percentage / %	I_D / I_G
NG-1	0.80	0.96
NG-2	4.71	1.06
NG-3	7.40	1.13
NG-4	7.04	1.11
NG-5	7.63	1.16

2.1.4　FT-IR analysis

The species of surface functional groups of GO and NG are characterized by using FT-IR spectroscopy (Fig.4). As can be seen from Fig.4, the GO showed distinct peaks at 3 423, 1 627, 1 417, and 1 126 cm^{-1}, which could be ascribed to hydroxyl stretching vibration, aromatic C=C, carboxyl O=C-O
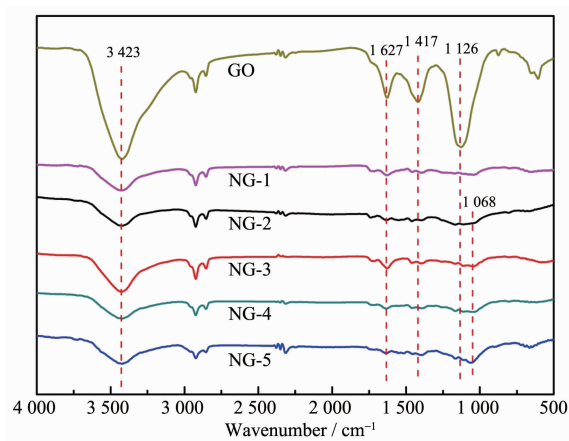
Fig.4　FT-IR spectra of GO, NG-1, NG-2, NG-3, NG-4
and NG-5 samples

and C-O[12,38-39]. After microwave solvothermal process, the contents of oxygen-function groups in NG significantly decreased, while a new nitrogen-related peak appeared at 1 068 cm⁻¹ in the FT-IR spectrum, which can be attributed to C-N[40]. The results suggest that the ED molecules can be successfully induced on the surface of graphene.

2.1.5　XPS analysis

　　XPS characterization was a powerful tool to analyze the elemental compositions and the state of imbedded nitrogen atoms within the graphene sheets. The binding energy at 284.6, 399.4 and 532.3 eV can be assigned to C1s, N1s and O1s, respectively. As shown in Fig.5, the O1s peaks of NG became significantly weaker and C1s peaks became much stronger than GO. The various N species contents of NG catalysts are listed in Table 2. Based on the analysis, presumably, N content depends on the ratio of EG and ED in microwave solvothermal process to a great extent. Interestingly, oxygen atomic percentage of NG-3 was decreased to 8.56% and the nitrogen atomic

percentage was increased to 7.63%, indicating oxygen functional in graphene crystal lattice were replace by N atoms in microwave solvothermal process[41-42]. Meanwhile, the above analysis has also revealed that the degree of graphene defect is depended on the content of doped nitrogen actually. The high-resolution C1s XPS spectra (Fig.6a) of GO corresponds to the carbon atoms in different functional groups: C-C (284.6 eV), C-O (286.8 eV) and C=O (287.8 eV). Significantly, the peak intensities of oxygen-containing groups became much weaker in NG. It is worth noting that an additional component appeared at 285.8 eV (Fig.6a and 6b), which can be attributed to the C-N bond[43]. These results are consistent with FT-IR (Fig.4) and XPS elemental analysis (Table 2). The bonding configurations of N atoms in NG were characterized by high-resolution N1s spectra (Fig.6c~6f), the NG can be fitted into three peaks at 398.3, 399.3 and 399.9 eV[44], which correspond to pyridine N, pyrrole N and graphitic N, respectively. The pyridinic N occurs in six-member ring and can
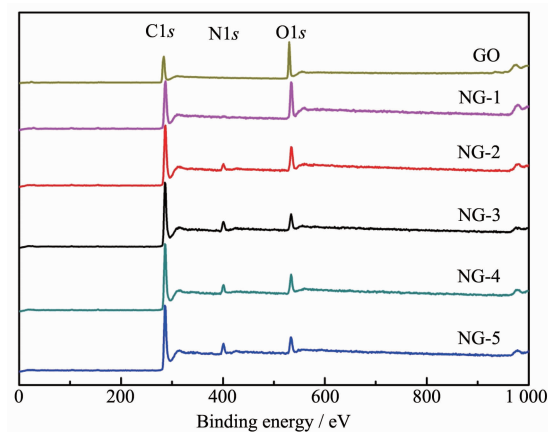

Fig.5　XPS spectra of GO, NG-1, NG-2, NG-3, NG-4
and NG-5 samples

**Table 2　Elemental composition (%, atomic percentage) of GO, NG-1, NG-2, NG-3, NG-4 and NG-5
samples and contents of pyridine, pyrrole, and graphite N by XPS**

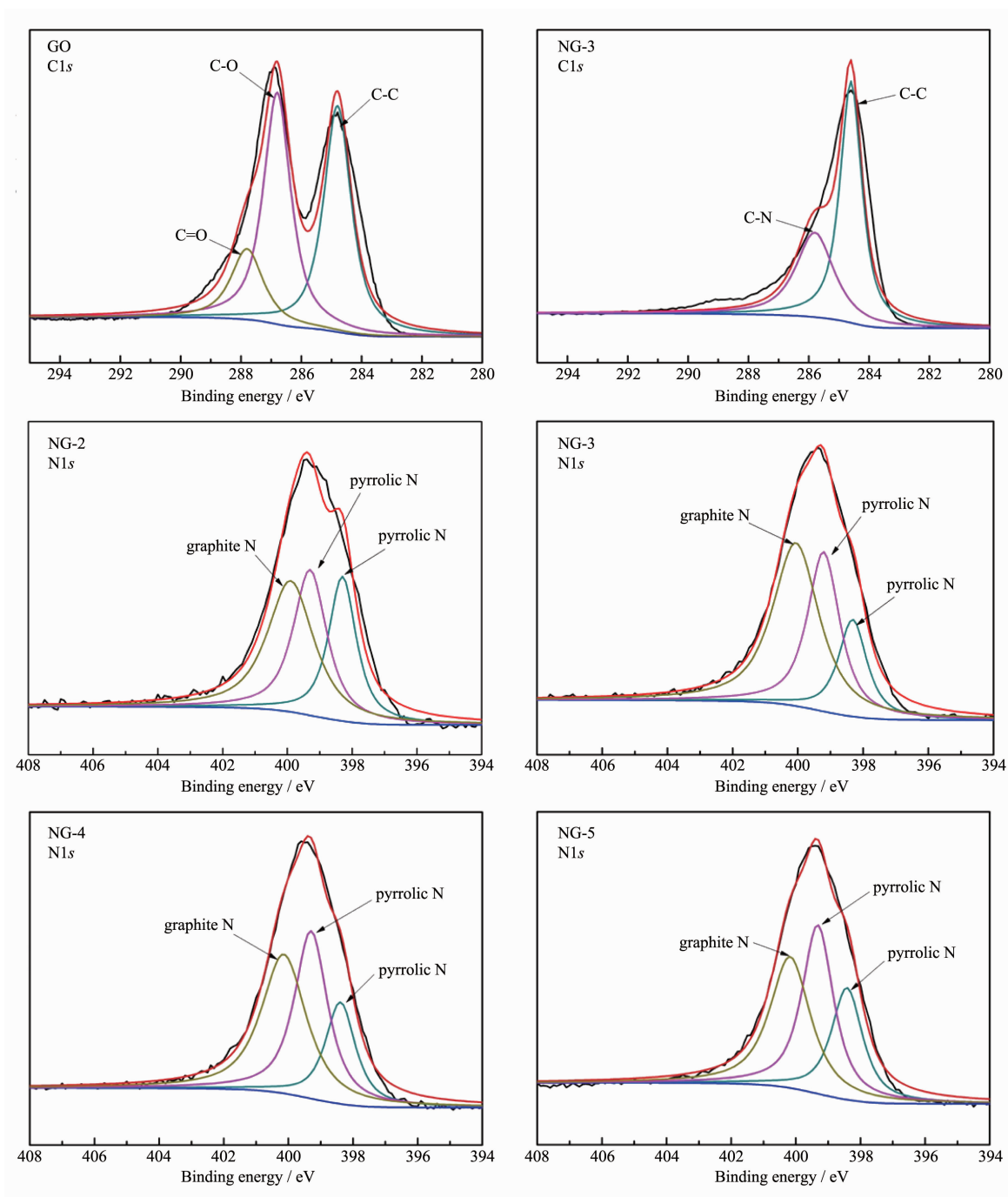| Sample	C	N	O	Pyridine N	Pyrrole N	Graphite N
GO	74.78	—	25.22	—	—	—
NG-1	78.84	0.80	20.36	—	—	—
NG-2	82.58	4.71	12.71	1.27	1.54	1.91
NG-3	84.04	7.40	8.56	1.33	2.46	3.61
NG-4	83.22	7.04	9.74	1.46	2.65	2.94
NG-5	83.38	7.63	8.99	1.89	2.88	2.86

Fig.6　C1*s* spectra of (a) GO, (b) NG-3 samples and N1*s* spectra of (c) NG-2, (d) NG-3, (e) NG-4, (f) NG-5 samples

donate one electron to the aromatic π system [10]. Pyrrolic N occurs in five-member ring and can contribute to the π-conjugated system in the graphene layers with two *p*-electrons [10]. Graphite N corresponds to N atoms that are linked with three carbon atoms in graphene basal plane, replacing the C atoms in graphene hexagonal ring[24-25]. From Table 2, it is clearly that, with increasing the amount of ED,

the content of graphite N increases firstly and reaches a maximum value in NG-3 catalyst, and then decreases beyond that point. As mentioned above, it is turned out that graphite N was doped into the graphene network and become saturated when V_{EG} : $V_{ED}=1:1$, but the excess N content may lead to the damages of graphene structure and more formation of edge-site. Such, the site of graphite N become less

and more opportunity for pyridinic N and pyrrolic N. Simultaneously, the variation tendency of E_{ORR} is similar to the content of graphite N. As a result, the values of E_{ORR} increase (*i.e.*, from −0.113 to −0.045 V) and reach a maximum value at NG-3, and then decline. It could be concluded that the graphite N plays an important role in ORR, which is consistent with previous research[29,32,46-48].

2.2 Electrocatalytic properties of NG towards ORR

2.2.1 Influence of different microwave solvothermal time towards ORR

Fig.7 showed the catalytic performance under handling for different microwave solvothermal times (V_{EG}:V_{ED}=1:1) on working electrode. The LSV measure-

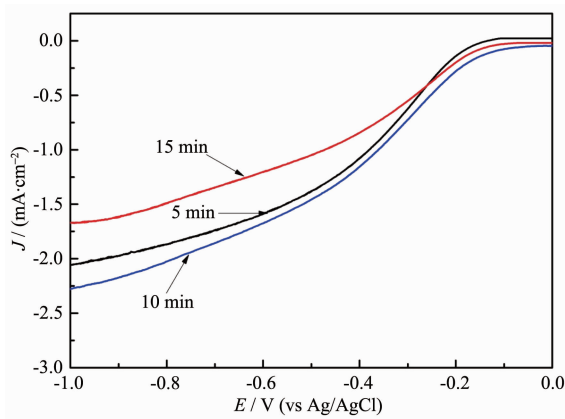ments were performed using 0.1 mol·L⁻¹ KOH aqueous solution with saturation oxygen between −1.0 and 0.0 V (vs Ag/AgCl). As described in Fig.7, when microwave solvothermal times were 5, 10 and 15 min, the catalysts showed different E_{ORR}: −0.106, −0.045 and −0.102 V, respectively. The E_{ORR} was markedly greater with 10 min. So, 10 min is chosen as the optimum microwave time for the further study.

2.2.2 Influence of difference ratio of EG and ED towards ORR

The compared results of LSVs of NG-1~NG-5 in 0.1 mol·L⁻¹ KOH aqueous solution with saturated oxygen at the rotation rate of 1 600 r·min⁻¹ were shown in Fig.8. The onset potentials for the ORR (E_{ORR}) of NG-1 ~NG-5 were −0.113, −0.105, −0.045, −0.054

Fig.7　LSV curves of different microwave solvothermal time (5, 10 and 15 min) in an O₂-saturated 0.1 mol·L⁻¹ KOH solution at a scanning rate of 10 mV·s⁻¹ and a rotation speed of 1 600 r·min⁻¹
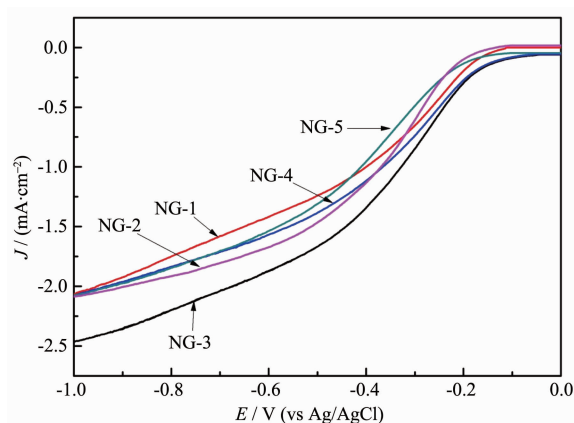
Fig.8　LSV curves of NG-1, NG-2, NG-3, NG-4 and NG-5 electrodes in an O₂-saturated 0.1 mol·L⁻¹ KOH solution at a scanning rate of 10 mV·s⁻¹ and a rotation speed of 1 600 r·min⁻¹
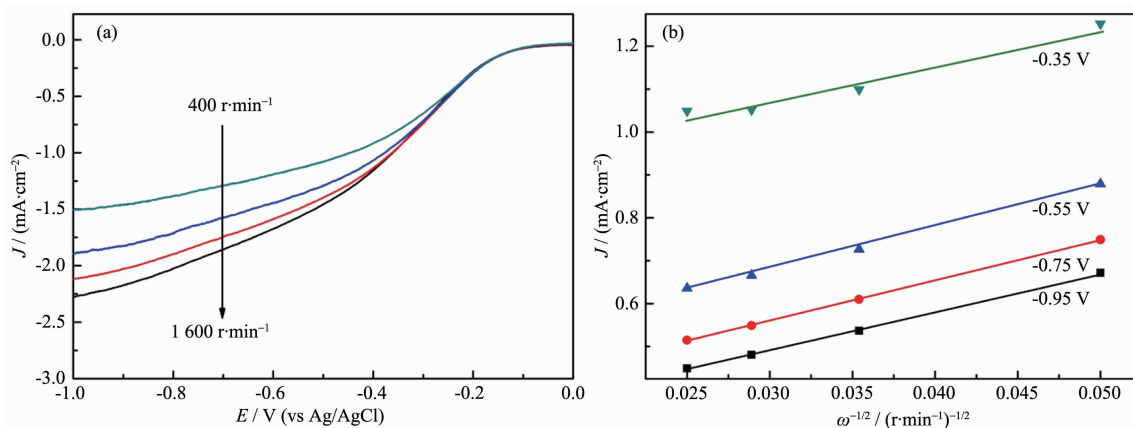
Fig.9　(a) RDE curves of NG-3 electrode in an O₂-saturated 0.1 mol·L⁻¹ KOH solution with different rotation speeds (400, 800, 1 200, 1 600 r·min⁻¹) at a scanning rate of 10 mV·s⁻¹; (b) K-L plots at different electrode potentials derived from RDE measurement

and −0.101 V, respectively. Compared to the other NG samples, NG-3 exhibited shifts positive of E_{ORR} and the larger current density. Combining the results of XPS, there were a marked effect between the ORR performance of NG and the content of graphite N, E_{ORR} gradually increased with the graphite N.

Fig.9a revealed RDE measurements results at different rotating speeds for NG-3, and the corresponding K-L plots at different electrode potentials were shown in Fig.9b. It was obviously that the K-L plots exhibited good linearity. The number of electrons transferred per oxygen molecule in NG-3 was calculated to be 3.2 ~3.5 electrons over the potential range from −0.35 to −0.95 V on the basis of the K-L equation. The results indicated that the ORR at NG-3 is a combinatorial process of two-electron and four-electron reactions.

3　Conclusions

In summary, we report a non-metal N-graphene catalyst with high performance by microwave solvo-thermal method using ED as the nitrogen source. The GO was reduced and doped by ED simultaneously. Consequently, the enhanced performance than the non-N-graphene sample can be attributed to the content of graphite N. However, excess content of N atoms may bring lager defect densities in micros-tructure which may induce adverse effects. The N atom percentage of NG-3 can be adjusted up to 7.40% as estimated by XPS analysis, and the atom percentage of graphite-N can be adjusted up to 3.61%. The NG-3 catalyst exhibited excellent activity with higher E_{ORR} and nearly a four-electron pathway in alkaline solution. Furthermore it indicates that NG material is a promising nanostuctured carbon material for advanced fuel cells.

References:

[1] Bashyam R, Zelenay P. *Nature*, **2006**,**443**(7107):63-66

[2] Jasinski R. *Nature*, **1964**,**201**(4925):1212-1213

[3] Stamenkovic V R, Fowler B, Mun B S, et al. *Science*, **2007**, **315**(5811):493-497

[4] Guo S J, Dong S J, Wang E. *ACS Nano*, **2010**,**4**(1):547-555

[5] Chen S G, Wei Z D, Qi X Q, et al. *J. Am. Chem. Soc.*, **2012**, **134**(32):13252-13255

[6] Markovic N M, Schmidt T J, Stamenkovic V, et al. *Fuel Cells*, **2001**,**1**(2):105-116

[7] Sun S H, Zhang G X, Geng D S, et al. *Angew. Chem.*, **2011**, **123**(2):442-446

[8] Mazumder V, Chi M, More K L, et al. *J. Am. Chem. Soc.*, **2010**,**132**(23):7848-7849

[9] Sebastián D, Ruíz A G, Suelves I, et al. *Appl. Catal. B*: *Environ.*, **2012**,**115**:269-275

[10]Sheng Z H, Shao L, Chen J J, et al. *ACS Nano*, **2011**,**5**(6): 4350-4358

[11]Zheng B, Wang J, Wang F B, et al. *Electrochem. Commun.*, **2013**,**28**:24-26

[12]Zhang C Z, Hao R, Liao H B, et al. *Nano Energy*, **2013**,**2** (1):88-97

[13]Alt H, Binder H, Sandstede G. *J. Catal.*, **1973**,**28**(1):8-19

[14]Liu R L, Wu D Q, Feng X L, et al. *Angew. Chem.*, **2010**, **122**(14):2619-2623

[15]Gong K P, Du F, Xia Z H, et al. *Science*, **2009**,**323**(5915): 760-764

[16]Li Y B, Zhang H M, Liu P R, et al. *Electrochem. Commun.*, **2015**,**51**:6-10

[17]Tian J Q, Ning R, Liu Q, et al. *ACS Appl. Mater. Inter.*, **2014**,**6**(2):1011-1017

[18]Liao Y L, Gao Y, Zhu S M, et al. *ACS Appl. Mater. Inter.*, **2015**,**7**(35):19619-19625

[19]Sheng Z H, Gao H L, Bao W J, et al. *J. Mater. Chem.*, **2012**, **22**(2):390-395

[20]Yang Z, Yao Z, Li G F, et al. *ACS Nano*, **2011**,**6**(1):205-211

[21]Zhang C Z, Mahmood N, Yin H, et al. *Adv. Mater.*, **2013**,**25** (35):4932-4937

[22]Zhang L P, Xia Z H. *J. Phys. Chem. C*, **2011**,**115**(22):11170-11176

[23]Groves M N, Chan A S W, Malardier-Jugroot C, et al. *Chem. Phys. Lett.*, **2009**,**481**(4):214-219

[24]Wang H B, Maiyalagan T, Wang X. *ACS Catal.*, **2012**,**2**(5): 781-794

[25]Fujita S I, Yamada K, Katagiri A, et al. *Appl. Catal., A*, **2014**,**488**:171-175

[26]Cong H P, Wang P, Gong M, et al. *Nano Energy*, **2014**,**3**: 55-63

[27]Wei D C, Liu Y Q, Wang Y, et al. *Nano Lett.*, **2009**,**9**(5): 1752-1758

[28]Long D H, Li W, Ling L C, et al. *Langmuir*, **2010**,**26**(20): 16096-16102

[29]Geng D S, Chen Y, Chen Y G, et al. *Energy Environ. Sci.*, **2011**,**4**(3):760-764

[30]Tian Y, Ye Y F, Wang X J, et al. *Appl. Catal., A*, **2017**,**529**:

127-133

[31]Murugan A V, Muraliganth T, Manthiram A. *Chem. Mater.*, **2009**,**21**(21):5004-5006

[32]Wang Z W, Li B, Xin Y C, et al. *Chin. J. Catal.*, **2014**,**35**(4):509-513

[33]WANG Kai(王凯), JI Bing-Cheng(季炳成), HAN Mei-Jia(韩美佳), et al. *Chinese J. Inorg. Chem.*(无机化学学报), **2013**,**29**(10):2105-2109

[34]Deng D H, Pan X L, Yu L, et al. *Chem. Mater.*, **2011**,**23**(5):1188-1193

[35]Guo H L, Su P, Kang X F, et al. *J. Mater. Chem. A*, **2013**,**1**(6):2248-2255

[36]Das A, Pisana S, Chakraborty B, et al. *Nat. Nanotechnol.*, **2008**,**3**(4):210-215

[37]Konstantin N K, Bulent O, Hannes C S, et al. *Nano Lett.*, **2008**,**8**(1):36-41

[38]Wu P, Qian Y D, Du P, et al. *J. Mater. Chem.*, **2012**,**22**(13):6402-6412

[39]Mo Z Y, Zheng R P, Peng H L, et al. *J. Power Sources*, **2014**,**245**:801-807

[40]Lin Z Y, Waller G, Liu Y, et al. *Adv. Energy. Mater.*, **2012**,**2**(7):884-888

[41]Zhang L S, Liang X Q, Song W G, et al. *Phys. Chem. Chem. Phys.*, **2010**,**12**(38):12055-12059

[42]Hu H, Zhao Z B, Zhou Q, et al. *Carbon*, **2012**,**50**(9):3267-3273

[43]Stankovich S, Dikin D A, Piner R D, et al. *Carbon*, **2007**,**45**(7):1558-1565

[44]Jiang B J, Tian C G, Wang L, et al. *Appl. Surf. Sci.*, **2012**,**258**(8):3438-3443

[45]Yang Z, Nie H G, Chen X H, et al. *J. Power Sources*, **2013**,**236**:238-249

[46]Lin Z Y, Waller G H, Liu Y, et al. *Nano Energy*, **2013**,**2**(2):241-248

[47]Lin Z Y, Song M K, Ding Y, et al. *Phys. Chem. Chem. Phys.*, **2012**,**14**(10):3381-3387

[48]Sidik R A, Aderson A B, Subramanian N P, et al. *J. Phys. Chem. B*, **2006**,**110**(4):1787-1793